Supplementary Materials for

Modelling the population-level protection conferred by COVID-19 vaccination

Pranesh Padmanabhan[1,*], Rajat Desikan[2,‡], Narendra M. Dixit[2,3,*]

[1]Clem Jones Centre for Ageing Dementia Research, Queensland Brain Institute, The University of Queensland, Brisbane, Australia 4072

[2]Department of Chemical Engineering, Indian Institute of Science, Bangalore, India 560012

[3]Centre for Biosystems Science and Engineering, Indian Institute of Science, Bangalore, India 560012

[‡]Current Address: Certara QSP, Certara UK Limited, Sheffield, UK

[*]Correspondence:

Pranesh Padmanabhan, Narendra M. Dixit

Email: p.padmanabhan@uq.edu.au; narendra@iisc.ac.in

This PDF file includes:

Materials and Methods

Data

We considered data from studies that reported *in vitro* dose-response curves of NAbs using SARS-CoV-2 pseudotyped virions (*5, 6, 31-47*). The assays estimated the fraction of infection events unaffected by the NAbs as a function of the NAb concentration (Fig. 1, and figs. S2 and S3). Data from such assays have been successfully used to estimate m and IC_{50} of antibodies against HIV-1 (*12*) and HCV (*13*). We extracted the data using Engauge Digitizer 12.1 and ensured consistency with reported details, such as dilution levels used.

Analysis of DRCs

We used both the standard sigmoidal dose-response curve equation (Eq. [1]) and the median-effect equation (Eq. [2]) to analyse the data.

$$f_u = 1 - f_a = \frac{(IC_{50})^m}{(D)^m + (IC_{50})^m} \quad (1)$$

$$\log_{10}\left(\frac{f_a}{f_u}\right) = m\log_{10}\left(\frac{D}{IC_{50}}\right) \quad (2)$$

Here, f_u and f_a are the fraction of infection events unaffected and affected by the NAbs in a single round of infection, D is the NAb concentration, IC_{50} is the half-maximal inhibitory concentration and m is the slope. Data was fitted using the tool NLINFIT in MATLAB R2017b. Data points with 1% < f_u < 99% were considered for parameter estimation. We fit the data using Eq. [1] and Eq. [2] separately and obtained estimates of IC_{50} and m for each NAb as well as associated 95% confidence intervals. We then computed

$IIP_{100} = \log_{10}\left(1+\left(\frac{100}{IC_{50}}\right)^{m}\right)$ using the estimates obtained using Eq. [1] and Eq. [2]. In most cases, the IIP_{100} values were close to each other. We did not include NAbs for which IIP_{100} values estimated using the two methods deviated by 20% or more in our analysis (table S1), for the deviation indicated that such NAbs either did not conform to the trends expected by Eqs. [1] and [2] or had large uncertainties in the data precluding robust parameter estimation. The details of the NAbs and parameter estimates are presented in table S1.

In silico simulation of plasma dilution assays

We simulated plasma dilution experiments as follows. We assumed that the plasma contained *N* NAbs with equimolar concentrations sampled from the landscape (Fig. 2A). The reciprocal plasma dilution curve was predicted assuming Loewe additivity (Eq. 3) or Bliss independence (Eq. [4]) between the different NAbs (*48-50*) using

$$\sum_{i=1}^{N}\frac{D_i/g}{IC_{50_i}\left(\frac{1}{e_L}-1\right)^{-1/m_i}}=1 \qquad (3)$$

$$e_B = 1-\prod_{i=1}^{N}\frac{\left(IC_{50_i}\right)^{m_i}}{\left(IC_{50_i}\right)^{m_i}+\left(D_i/g\right)^{m_i}} \qquad (4)$$

Here, g is the plasma dilution factor. e_L and e_B are the fractions of infection events affected by the plasma in a single round of infection estimated using Loewe additivity and Bliss independence, respectively. D_i is the concentration of the i^{th} NAb in the plasma before dilution, IC_{50_i} is its half-maximal inhibitory concentration and m_i its slope, with

$i \hat{1} \{1,2,..,N\}$. We let N = 10 in our simulations, based on the number of NAbs with significant neutralization efficacy seen in patients (*5*). We estimated the value of g at which $e = 0.5$ as the corresponding NT_{50}. We chose D_i as D_0 /N, and varied D_0 between 0.1 and100 µg/ml.

We repeated these simulations 100 times at different NAb titres, with each simulation representative of an individual patient. We compared the resulting predictions at D_0 = 30 µg/ml with observations from 3 patients (Fig. 3C) (*15*), which also we digitized (Fig. 3B). The equation $f_u = \frac{(g)^n}{(g)^n + (NT_{50})^n}$ was fit to the observations from 3 patients. Here, n is the Hill coefficient, g is the plasma dilution and NT_{50} is the half-maximal inhibitory plasma neutralizing titre. We also compared predictions of the dependence of NT_{50} on NAb titres with experimental observations (Fig. 3D) (*17*).

Model of SARS-CoV-2 dynamics post-vaccination

To predict the protection conferred by vaccines, we developed a mathematical model of within-host SARS-CoV-2 infection post-vaccination. We adapted previous models (*24, 51-54*) by focussing on early dynamics, required to accurately predict the reduction in the peak viral load due to pre-existing NAbs. The following equations described the resulting infection dynamics in vaccinated individuals exposed to the virus:

$$\frac{dT}{dt} = -b(1-e)VT - r_X XT \quad (5)$$

$$\frac{dR}{dt} = \rho_X XT \quad (6)$$

$$\frac{dI}{dt} = \beta(1-\varepsilon)VT - \delta I \quad (7)$$

$$\frac{dV}{dt} = pI - cV \quad (8)$$

$$\frac{dX}{dt} = \frac{\sigma_X I(1-X)}{f_X + I} - d_X X \quad (9)$$

Here, uninfected target cells, T, are infected by SARS-CoV-2 virions, V, with the second order rate constant β, producing infected cells, I. Cells I produce virions at the rate p per cell and are lost with a rate constant δ. The virions are cleared with a rate constant c. The activation of the innate immune response, quantified phenomenologically using X, is assumed to be a saturable function of I, with the maximal rate σ_X and the half-maximal activation parameter f_X. If I is not limiting, X would rise at the rate σ_X at low X and cease to rise as X approaches 1. X converts uninfected cells to an infection-refractory state, R, at a per capita rate r_X and decays with a rate constant d_X. The pre-existing NAbs are drawn as random subsets from the landscape (Fig. 2A) to block new infections with an efficacy ε, which is a function of NAb titre and computed using Eq. [1] or Eq. [2].

To examine the variation in peak viral loads with NAb titres (Fig. 4C), we predicted viral dynamics of 3500 infected individuals, each individual with different pre-existing NAbs sampled from the landscape as well as different values of the viral dynamics parameters (table S2). To obtain the protection curve (Fig. 4D), we simulated viral dynamics in 2000 virtual individuals, as we described above, and obtained peak viral loads. Further, for each individual, we also simulated plasma dilution assays and estimated NT_{50}. We then binned individuals into narrow ranges of NT_{50} values. In each bin, we estimated the fraction

of individuals with peak viral load below 100 copies/ml. This fraction yielded the protection curve. The error bars (standard deviation) of the protection curve were obtained from 5 independent realizations.

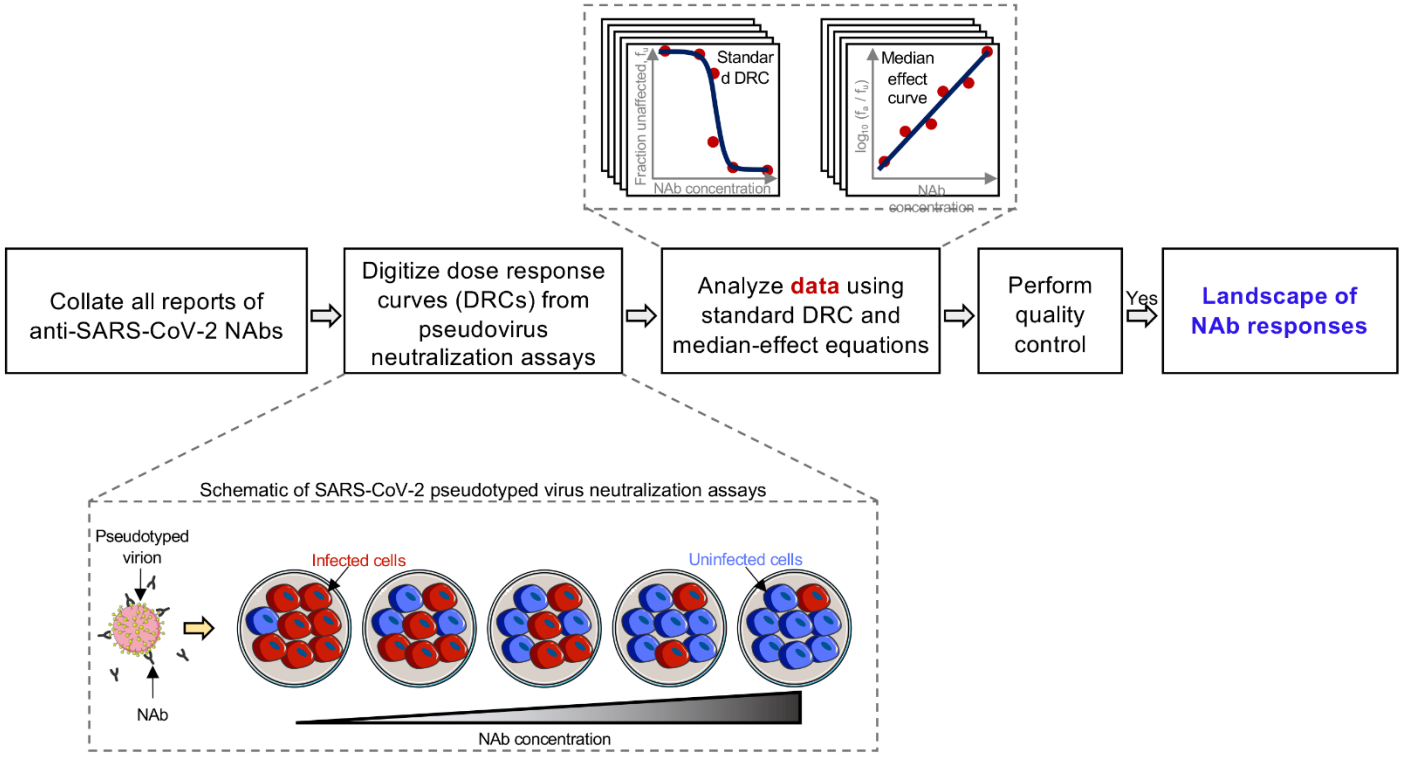

Fig. S1. Schematic of the workflow to chart out the quantitative landscape of SARS-CoV-2 NAbs. We collated data from a large number of studies that reported DRCs of NAbs using SARS-CoV-2 pseudotyped virions. The assays estimate the fraction of infection events affected/unaffected by the NAbs as a function of the NAb concentration. We extracted and analysed the data using both the standard DRC equation (Eq. [1]) and the median-effect equation (Eq. [2]) to estimate IC_{50} and m. We then computed $IIP_{100} = \log_{10}\left(1+\left(\frac{100}{IC_{50}}\right)^{m}\right)$ using the estimates obtained by both equations. NAbs with consistent estimates were considered for rank-ordering.

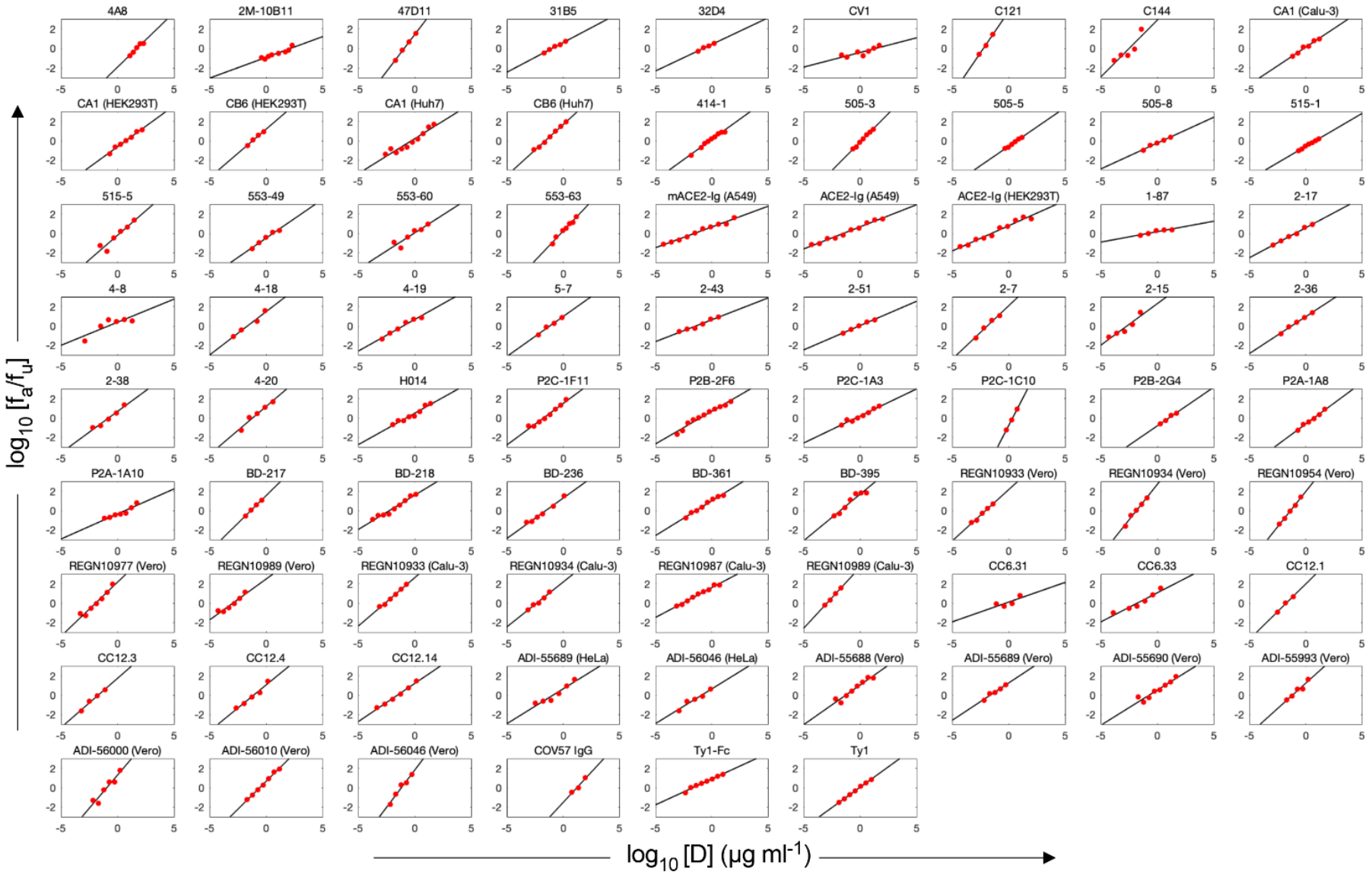

Fig. S2. Estimates of IC_{50} and m of SARS-CoV-2 NAbs using the median-effect equation. Fits (lines) of the median-effect equation to published experimental data (circles). Experimental data points with 1% < f_u < 99% (filled circles) were considered for parameter estimation.

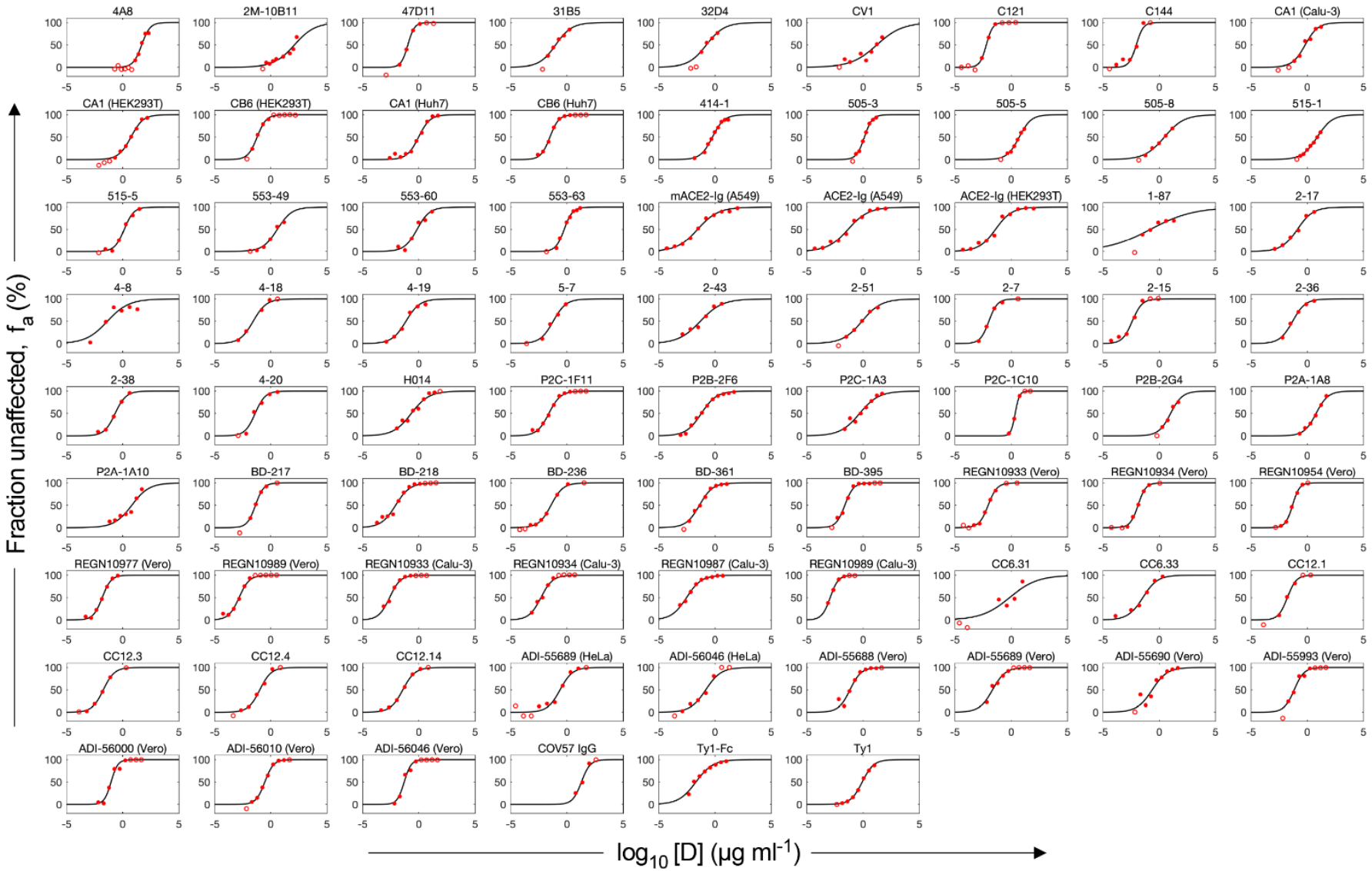

Fig. S3. Estimates of IC_{50} and m of SARS-CoV-2 NAbs using the standard dose-response curve equation. Fits (lines) of the standard dose-response curve equation to published experimental data (circles). Experimental data points with 1% < f_u < 99% (filled circles) were considered for parameter estimation.

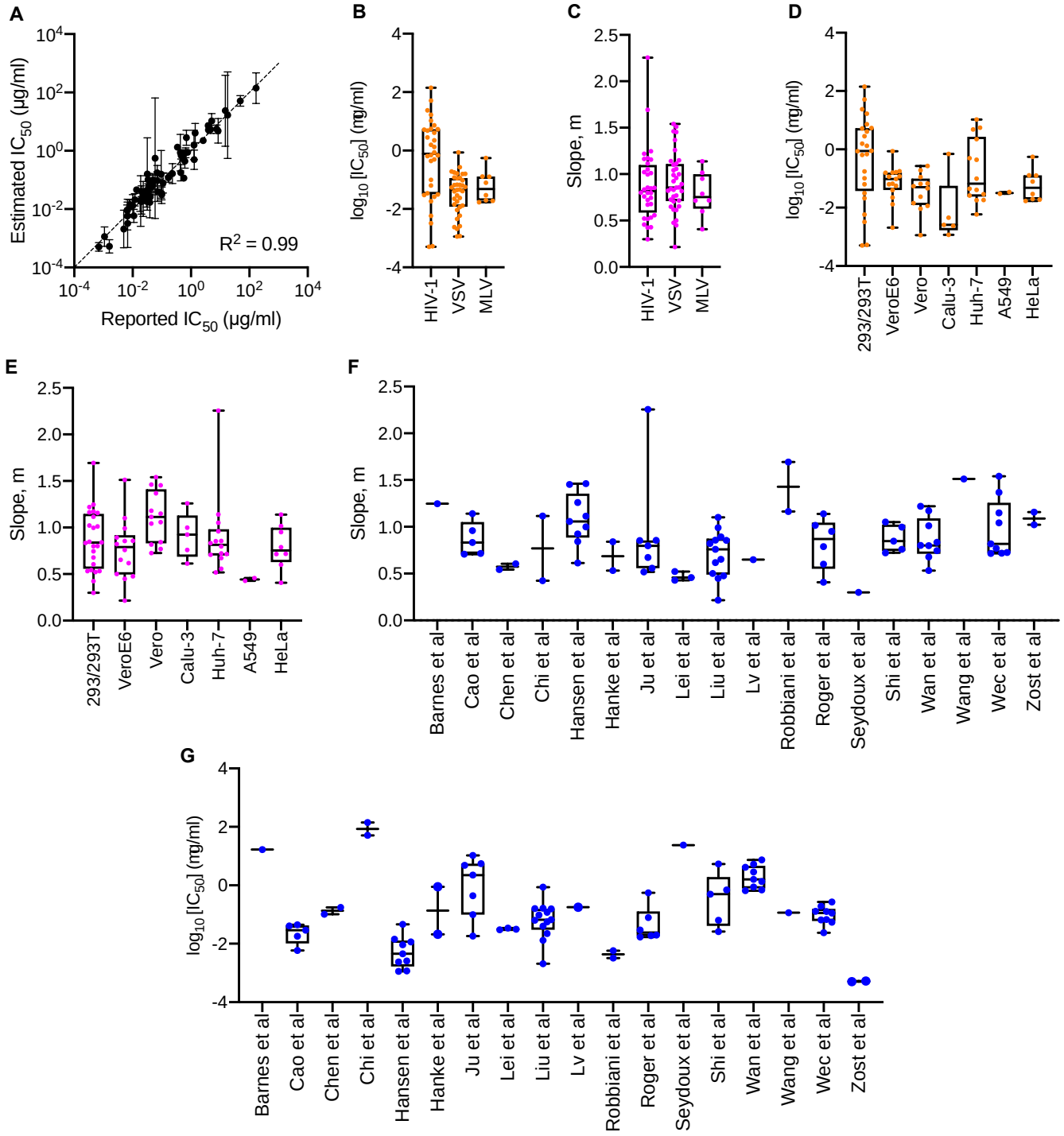

Fig. S4. Robustness of the estimates of IC_{50} and m of SARS-CoV-2 NAbs. (A) Comparison of the estimated and reported values of IC_{50} (see table S1). Error bars are 95% confidence intervals. (B, C) Variability in m (B) and IC_{50} (C) within different studies (see table S1 for details of the studies).

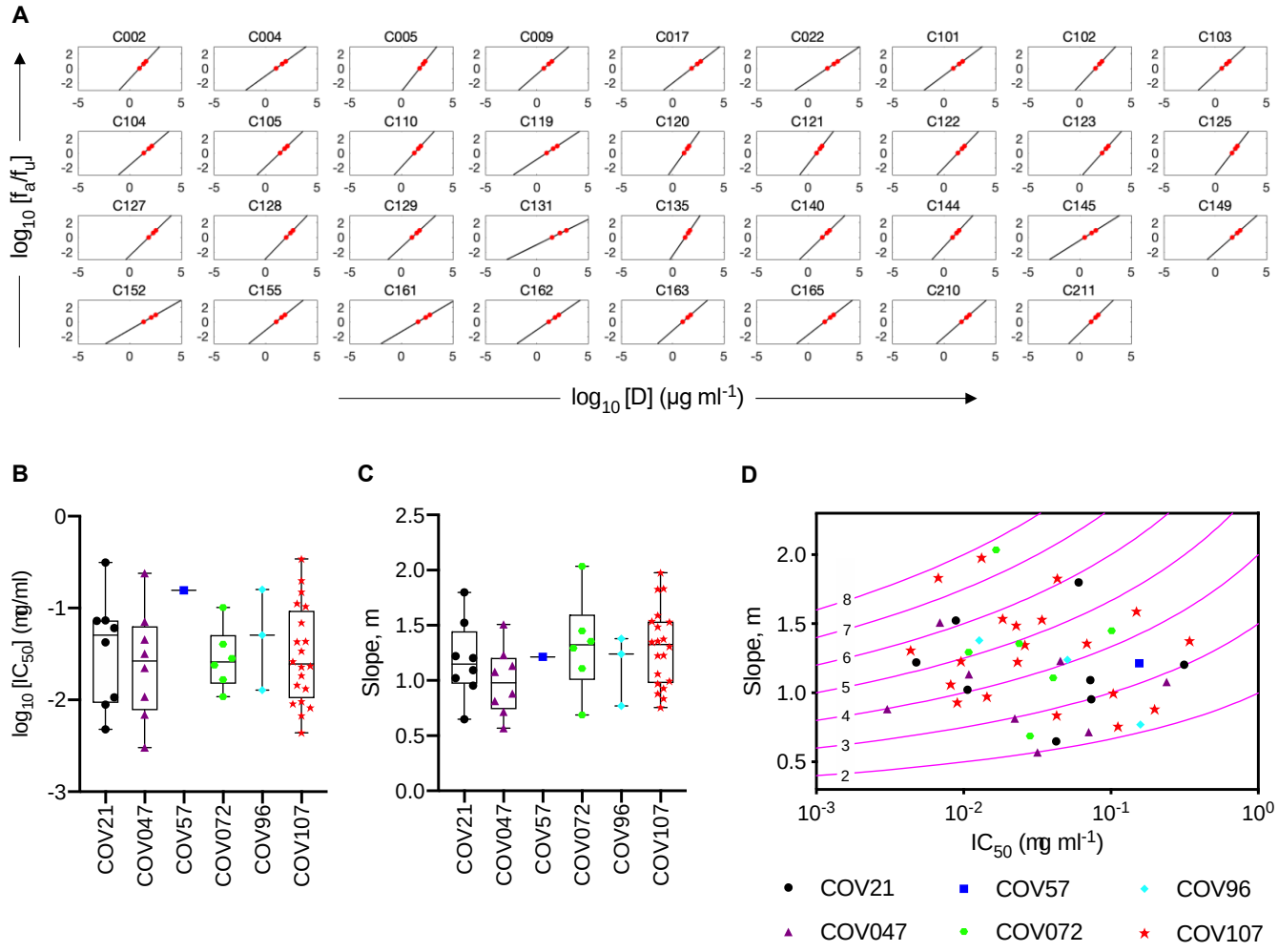

Fig. S5. Estimates of IC_{50} and m of SARS-CoV-2 NAbs from patients. (A) Fits (lines) of the median-effect equation to published experimental data (circles) reporting IC_{50}, IC_{80} and IC_{90} for NAbs drawn from eight patients (*6*). For some NAbs, only IC_{50} and IC_{80} were available. The slopes for these latter NAbs were estimated using the equation $m = \frac{\log_{10}(4)}{\log_{10}(IC_{80}) - \log_{10}(IC_{50})}$ derived from the median-effect equation (Eq. [2]). The corresponding best-fit estimates of (B) IC_{50} and (C) m are shown along with (D) the location of the NAbs on the landscape.

Table S1. Best-fit estimates of dose-response curve parameters of NAbs.

Data					Fits and predictions					
					Median-effect equation			Standard dose response curve		
Antibody	Cell line	Viral backbone	Reported IC_{50}	Ref	m (95% CI)	IC_{50} (95% CI)	IIP_{100}	m (95% CI)	IC_{50} (95% CI)	IIP_{100}
4A8	293T/ACE2	HIV-1	49 μg/ml	(*31*)	1.12 (0.64, 1.59)	51.29 μg/ml (33.75, 77.96)	0.49	1.17 (0.61, 1.73)	48.06 μg/ml (33.09, 69.81)	0.53
2M-10B11	293T/ACE2	HIV-1	170 μg/ml	(*31*)	0.42 (0.28, 0.57)	140.51 μg/ml (41.89, 471.27)	0.27	0.48 (0.26, 0.7)	126.72 μg/ml (52.48, 305.96)	0.28
47D11	VeroE6	VSV	0.57 μg/ml	(*32*)	1.51 μg/ml (1.29, 1.74)	0.12 μg/ml (0.09, 0.15)	4.44	1.48 (1.15, 1.81)	0.11 μg/ml (0.09, 0.13)	4.39
31B5	293T/ACE2	-	0.034 μg/ml	(*46*)	0.61 (0.48, 0.73)	0.1 μg/ml (0.07, 0.14)	1.81	0.6 (0.45, 0.76)	0.1 μg/ml (0.07, 0.14)	1.82
32D4	293T/ACE2	-	0.07 μg/ml	(*46*)	0.54 (0.31, 0.77)	0.18 μg/ml (0.1, 0.32)	1.51	0.55 (0.27, 0.82)	0.17 μg/ml (0.09, 0.31)	1.52
CV1	293T/ACE2	HIV-1	15 μg/ml	(*33*)	0.3 (0.08, 0.52)	23.67 μg/ml (1.44, 390.2)	0.4	0.38 (0.11, 0.66)	16.96 μg/ml (3.88, 74.12)	0.47
CV30[$]	293T/ACE2	HIV-1	0.03 μg/ml	(*33*)	0.91 (0.51, 1.31)	0.03 μg/ml (0.01, 0.1)	3.17	1.19 (0.7, 1.68)	0.04 μg/ml (0.03, 0.06)	4.05
C121[#]	293T/ACE2	HIV-1	6.7 ng/ml	(*6*)	1.69 (0.19, 3.2)	5.81 ng/ml (1.92, 17.56)	7.17	1.54 (0.17, 2.91)	6.09 ng/ml (3.18, 11.65)	6.51
C135[$#]	293T/ACE2	HIV-1	16.5 ng/ml	(*6*)	0.87 (0.39, 1.35)	21.65 ng/ml (4.93-95.12)	3.2	1.91 (1.08, 2.75)	16.35 ng/ml (12.13, 22.03)	7.24

C144[*#]	293T/ACE2	HIV-1	6.8 ng/ml	(*6*)	1.16 (0.04, 2.28)	3.24 ng/ml (0.48, 21.74)	5.22	1.41 (0, 3.09)	9 ng/ml (3.64, 22.23)	5.69
CA1	Calu-3	HIV-1	0.53 μg/ml	(*34*)	0.76 (0.58, 0.94)	0.69 μg/ml (0.44, 1.09)	1.65	0.77 (0.47, 1.07)	0.64 μg/ml (0.39, 1.07)	1.69
CA1	293T/ACE2	HIV-1	4.66 μg/ml	(*34*)	0.85 (0.72, 0.97)	5.4 μg/ml (3.93, 7.41)	1.11	0.8 (0.68, 0.92)	5.22 μg/ml (4.26, 6.4)	1.07
CA1	Huh-7	HIV-1	1.28 μg/ml	(*34*)	0.72 (0.55, 0.9)	0.5 μg/ml (0.23, 1.06)	1.68	0.85 (0.64, 1.07)	0.95 μg/ml (0.68, 1.31)	1.74
CB6[$*]	Calu-3	HIV-1	0.02 μg/ml	(*34*)	1.33 (0.37, 2.28)	0.04 μg/ml (0.01, 0.13)	4.5	1.68 (0, 3.59)	0.03 μg/ml (0.01, 0.06)	6
CB6	293T/ACE2	HIV-1	0.04 μg/ml	(*34*)	1 (0.66, 1.33)	0.06 μg/ml (0.04, 0.1)	3.19	1.07 (0.68, 1.45)	0.06 μg/ml (0.04, 0.08)	3.44
CB6	Huh-7	HIV-1	0.04 μg/ml	(*34*)	1.05 (0.95, 1.15)	0.03 μg/ml (0.02, 0.03)	3.77	1.09 (0.93, 1.26)	0.03 μg/ml (0.03, 0.04)	3.85
414-1	293T/ACE2	HIV-1	3.09 nM	(*47*)	0.83 (0.73, 0.94)	4.54 nM (3.49, 5.91)	1.81	0.83 (0.72, 0.95)	3.89 nM (3.31, 4.58)	1.87
505-3	293T/ACE2	HIV-1	2.31 nM	(*47*)	1.17 (1.06, 1.29)	8.82 nM (7.67, 10.14)	2.2	1.25 (1.1, 1.39)	8.71 nM (7.88, 9.64)	2.35
505-5	293T/ACE2	HIV-1	26.37 nM	(*47*)	0.8 (0.68, 0.92)	34.67 nM (28.06, 42.84)	1.07	0.82 (0.69, 0.95)	34.1 nM (29.06, 40)	1.09
505-8	293T/ACE2	HIV-1	4.67 nM	(*47*)	0.53 (0.39, 0.67)	18.73 nM (10.35, 33.88)	0.89	0.5 (0.38, 0.62)	18.63 nM (12.68, 27.39)	0.84
515-1	293T/ACE2	HIV-1	26.11 nM	(*47*)	0.68 (0.61, 0.74)	48.56 nM (40.4, 58.35)	0.84	0.65 (0.59, 0.72)	49.49 nM (43.37, 56.47)	0.81

515-5	293T/ACE2	HIV-1	5.39/8.47 nM	(*47*)	1.01 (0.53, 1.5)	10.54 nM (3.3, 33.67)	1.83	1.04 (0.71, 1.37)	9.01 nM (6.41, 12.65)	1.95
553-49	293T/ACE2	HIV-1	9.26 nM	(*47*)	0.8 (0.55, 1.05)	27.13 nM (12.68, 58.04)	1.15	0.68 nM (0.36, 1.01)	25.35 (13.23, 48.59)	1.01
553-60	293T/ACE2	HIV-1	2.87 nM	(*47*)	0.75 (0.31, 1.18)	5.78 nM (1.37, 24.38)	1.55	0.78 (0.34, 1.21)	4.64 nM (2.13, 10.11)	1.69
553-63	293T/ACE2	HIV-1	3.57 nM	(*47*)	1.22 (1.02, 1.42)	4.32 nM (3.18, 5.85)	2.67	1.17 (0.93, 1.41)	3.8 nM (3.06, 4.73)	2.63
mACE2-Ig	A549/ACE2	HIV-1	0.03 μg/ml	(*36*)	0.43 (0.38, 0.47	0.03 μg/ml (0.02, 0.05)	1.52	0.47 (0.41, 0.54)	0.03 μg/ml (0.02, 0.04)	1.69
mACE2-Ig[$]	293T/ACE2	HIV-1	0.08 μg/ml	(*36*)	0.55 (0.44, 0.67	0.02 μg/ml (0.01, 0.05)	2.07	0.7 (0.53, 0.86)	0.02 μg/ml (0.02, 0.04)	2.52
ACE2-Ig	A549/ACE2	HIV-1	0.1 μg/ml	(*36*)	0.46 (0.41, 0.51	0.03 μg/ml (0.02, 0.06)	1.59	0.48 (0.38, 0.57)	0.05 μg/ml (0.03, 0.07)	1.6
ACE2-Ig	293T/ACE2	HIV-1	0.1 μg/ml	(*36*)	0.52 (0.44, 0.6)	0.03 μg/ml (0.02, 0.06)	1.83	0.59 (0.42, 0.77)	0.04 μg/ml (0.02, 0.07)	2.02
2-26[$]	VeroE6	VSV	-	(*5*)	0.36 (0.11, 0.62)	4.42 μg/ml (0.33, 60.08)	0.61	0.53 (0.16, 0.89)	3.58 μg/ml (1.03, 12.4)	0.83
1-68[$]	VeroE6	VSV	0.767 μg/ml	(*5*)	0.65 (0.001, 1.3)	1.68 μg/ml (0.03, 109.8)	1.18	0.7 (0.42, 0.98)	0.95 μg/ml (0.54, 1.66)	1.43
1-87	VeroE6	VSV	0.095 μg/ml	(*5*)	0.22 (0.07, 0.36)	0.16 μg/ml (0.02, 1.03)	0.7	0.23 (0.08, 0.38)	0.16 (0.03, 0.82)	0.72
2-17	VeroE6	VSV	0.168 μg/ml	(*5*)	0.62 (0.54, 0.69)	0.12 μg/ml (0.08, 0.17)	1.81	0.63 (0.47, 0.78)	0.13 μg/ml (0.08, 0.2)	1.81

4-8[*]	VeroE6	VSV	0.032 μg/ml	(5)	0.48 (0.05, 0.9)	0.16 μg/ml (0.01, 2.76)	1.35	0.46 (0, 0.92)	0.04 μg/ml (0.01, 0.42)	1.55
4-18	VeroE6	VSV	0.023 μg/ml	(5)	0.89 (0.41, 1.37)	0.02 μg/ml (0.01, 0.09)	3.26	0.74 (0.35, 1.13)	0.03 μg/ml (0.01, 0.08)	2.64
4-19	VeroE6	VSV	0.07 μg/ml	(5)	0.65 (0.49, 0.81)	0.1 μg/ml (0.05, 0.19)	1.97	0.71 (0.48, 0.94)	0.07 μg/ml (0.04, 0.12)	2.22
5-7	VeroE6	VSV	0.05 μg/ml	(5)	0.82 (0.47, 1.17)	0.07 μg/ml (0.03, 0.14)	2.61	0.76 (0.27, 1.25)	0.06 μg/ml (0.03, 0.14)	2.46
5-24[$]	VeroE6	VSV	0.013 μg/ml	(5)	0.3 (0.02, 0.58)	0.005 μg/ml (1×10^{-4}, 0.28)	1.3	0.4 (0.13, 0.66)	0.009 μg/ml (0.002, 0.04)	1.62
2-43	VeroE6	VSV	0.071 μg/ml	(5)	0.45 (0.32, 0.58)	0.04 μg/ml (0.02, 0.09)	1.54	0.45 (0.28, 0.62)	0.05 μg/ml (0.02, 0.11)	1.5
2-51	VeroE6	VSV	0.652 μg/ml	(5)	0.5 (0.42, 0.59)	0.86 μg/ml (0.58, 1.27)	1.08	0.51 (0.42, 0.6)	0.8 μg/ml (0.57, 1.12)	1.11
1-20[$*]	VeroE6	VSV	0.127 μg/ml	(5)	1.2 (0.18, 2.23)	0.06 μg/ml (0.01, 0.29)	3.85	0.87 (0, 2.08)	0.09 μg/ml (0.02, 0.47)	2.66
1-57[$]	VeroE6	VSV	0.009 μg/ml	(5)	0.97 (0.52, 1.42)	0.01 μg/ml (0.003, 0.03)	3.86	0.72 (0.3, 1.13)	0.01 μg/ml (0.005, 0.02)	2.86
2-4[$]	VeroE6	VSV	0.394 μg/ml	(5)	1.27 (0.28, 2.26)	0.58 μg/ml (0.14, 2.46)	2.84	0.92 (0.19, 1.66)	0.44 μg/ml (0.18, 1.12)	2.18
2-7	VeroE6	VSV	0.01 μg/ml	(5)	1.1 (0.57, 1.64)	0.01 μg/ml (0.005, 0.03)	4.28	1.15 (0.61, 1.68)	0.01 μg/ml (0.007, 0.02)	4.57
2-15	VeroE6	VSV	0.005 μg/ml	(5)	0.86 (0.31, 1.4)	0.002 μg/ml (0.001, 0.009)	4.01	1.01 (0.3, 1.72)	0.004 μg/ml (0.002, 0.009)	4.45

2-30[$]	VeroE6	VSV	0.512 μg/ml	(*5*)	0.87 (0.37, 1.36)	0.36 μg/ml (0.06, 2.23)	2.12	1.17 (0.92, 1.41)	0.46 μg/ml (0.38, 0.56)	2.73
2-36	VeroE6	VSV	0.044 μg/ml	(*5*)	0.76 (0.64, 0.88)	0.06 μg/ml (0.04, 0.08)	2.47	0.78 (0.58, 0.97)	0.05 μg/ml (0.04, 0.07)	2.57
2-38	VeroE6	VSV	0.232 μg/ml	(*5*)	0.86 (0.56, 1.15)	0.17 μg/ml (0.08, 0.36)	2.38	0.9 (0.64, 1.16)	0.21 μg/ml (0.15, 0.31)	2.41
4-20	VeroE6	VSV	0.036 μg/ml	(*5*)	0.99 (0.6, 1.38)	0.06 μg/ml (0.02, 0.17)	3.16	0.96 (0.25, 1.67)	0.04 μg/ml (0.02, 0.09)	3.27
H014 IgG	Vero	VSV	3 nM	(*37*)	0.65 (0.5, 0.8)	1.18 nM (0.62, 2.23)	1.79	0.55 (0.38, 0.72)	1.44 nM (0.83, 2.51)	1.48
COV2-2196	293/ACE2	HIV-1	0.7 ng/ml	(*38*)	1.16 (0.98, 1.33)	0.5 ng/ml (0.36, 0.7)	6.13	1.29 (1.11, 1.48)	0.4 ng/ml (0.35, 0.45)	6.99
COV2-2130	293/ACE2	HIV-1	1.6 ng/ml	(*38*)	1.02 (0.77, 1.27)	0.53 ng/ml (0.31, 0.9)	5.39	0.96 (0.28, 1.64)	0.62 ng/ml (0.29, 1.3)	5.01
P2C-1F11	Huh7	HIV-1	0.03 μg/ml	(*39*)	0.85 (0.71, 1)	0.02 μg/ml (0.01, 0.03)	3.19	0.83 (0.67, 0.99)	0.02 μg/ml (0.02, 0.03)	2.99
P2B-2F6	Huh7	HIV-1	0.05 μg/ml	(*39*)	0.67 (0.58, 0.76)	0.1 μg/ml (0.06, 0.16)	2.02	0.64 (0.55, 0.73)	0.06 μg/ml (0.05, 0.08)	2.07
P2C-1A3	Huh7	HIV-1	0.62 μg/ml	(*39*)	0.56 (0.44, 0.67)	0.44 μg/ml (0.25, 0.77)	1.33	0.51 (0.34, 0.67)	0.49 μg/ml (0.27, 0.9)	1.2
P2C-1C10	Huh7	HIV-1	2.62 μg/ml	(*39*)	2.25 (1.64, 2.87)	2.22 μg/ml (1.73, 2.86)	3.73	2.3 (1.47, 3.13)	2.26 μg/ml (1.93, 2.66)	3.79
P2B-2G4	Huh7	HIV-1	5.11 μg/ml	(*39*)	0.8 (0.43, 1.17)	10.57 μg/ml (5.95, 18.77)	0.85	0.82 (0.35, 1.3)	10.23 μg/ml (5.62, 18.62)	0.88

P2A-1A8	Huh7	HIV-1	7.68 μg/ml	(*39*)	0.85 (0.71, 1)	5.5 μg/ml (3.97, 7.6)	1.11	0.82 (0.65, 0.99)	6.01 μg/ml (4.64, 7.8)	1.04
P2A-1A10	Huh7	HIV-1	8.57 μg/ml	(*39*)	0.52 (0.31, 0.72)	4.83 μg/ml (1.84, 12.67)	0.76	0.56 (0.29, 0.84)	6.29 μg/ml (2.8, 14.14)	0.76
BD-217	Huh7	VSV	0.031 μg/ml	(*40*)	1.14 (0.95, 1.33)	0.05 μg/ml (0.04, 0.06)	3.82	1.19 (0.98, 1.4)	0.04 μg/ml (0.04, 0.05)	3.99
BD-218	Huh7	VSV	0.011 μg/ml	(*40*)	0.71 (0.59, 0.83)	0.006 μg/ml (0.004, 0.01)	2.99	0.68 (0.48, 0.89)	0.009 μg/ml (0.005, 0.01)	2.78
BD-236	Huh7	VSV	0.037 μg/ml	(*40*)	0.83 (0.67, 1)	0.03 μg/ml (0.02, 0.05)	2.94	0.81 (0.7, 0.92)	0.04 μg/ml (0.03, 0.05)	2.78
BD-361	Huh7	VSV	0.02 μg/ml	(*40*)	0.71 (0.62, 0.81)	0.04 μg/ml (0.03, 0.06)	2.42	0.74 (0.61, 0.87)	0.04 μg/ml (0.03, 0.05)	2.51
BD-368[$]	Huh7	VSV	0.035 μg/ml	(*40*)	0.72 (0.6, 0.84)	0.04 μg/ml (0.02, 0.08)	2.42	0.97 (0.79, 1.15)	0.04 μg/ml (0.03, 0.05)	3.3
BD-368-2[$]	Huh7	VSV	0.0012 μg/ml	(*40*)	1.16 (0.86, 1.46)	0.002 μg/ml (0.001, 0.003)	5.5	1.46 (1.33, 1.59)	0.0018 μg/ml (0.0017, 0.0019)	6.9
BD-395	Huh7	VSV	0.02 μg/ml	(*40*)	0.96 (0.64, 1.28)	0.02 μg/ml (0.01, 0.05)	3.59	1.13 (0.79, 1.47)	0.02 μg/ml (0.02, 0.03)	4.09
REGN10933	Vero	VSV	4.28 x 10^{-11} M	(*41*)	1.06 (0.81, 1.31)	6.17 x 10^{-11} M (4.11, 9.25) x 10^{-11}	4.27	1.1 (0.86, 1.34)	5.93 x 10^{-11} M (4.82, 7.29) x 10^{-11}	4.45
REGN10933	Calu-3	VSV	-	(*41*)	1.0 (0.86, 1.14)	1.58 x 10^{-11} M (1.11, 2.24) x 10^{-11}	4.62	0.9 (0.62, 1.19)	1.67 x 10^{-11} M (1.18, 2.36) x 10^{-11}	4.16
REGN10934	Vero	VSV	5.44 x 10^{-11} M	(*41*)	1.46 (1.09, 1.84)	9.62 x 10^{-11} M (6.45, 14.3) x 10^{-11}	5.61	1.28 (0.98, 1.57)	8.54 x 10^{-11} M (6.98, 10.5) x 10^{-11}	4.96

REGN10934	Calu-3	VSV	-	(*41*)	0.92 (0.64, 1.2)	3.01 x 10^{-11} M (1.85, 4.9) x 10^{-11}	4.01	0.83 (0.45, 1.2)	3.22 x 10^{-11} M (1.9, 5.44) x 10^{-11}	3.58
REGN10954	Vero	VSV	9.22 x 10^{-11} M	(*41*)	1.45 (1.28, 1.63)	3.07 x 10^{-10} M (2.55, 3.7) x 10^{-10}	4.85	1.41 (1.19, 1.63)	3.2 x 10^{-10} M (2.83, 3.62) x 10^{-10}	4.69
REGN10964[$]	Vero	VSV	5.7 x 10^{-11} M	(*41*)	1.02 (0.67, 1.36)	6.95 x 10^{-11} M (2.62, 18.4) x 10^{-11}	4.05	1.32 (1.15, 1.48)	9.25 x 10^{-11} M (8.32, 10.3) x 10^{-11}	5.07
REGN10977	Vero	VSV	5.15 x 10^{-11} M	(*41*)	1.11 (0.82, 1.41)	7.74 x 10^{-11} M (4.34, 13.8) x 10^{-11}	4.38	1.1 (0.89, 1.3)	1 x 10^{-10} M (0.83, 1.21) x 10^{-11}	4.19
REGN10984[$]	Vero	VSV	9.73 x 10^{-11} M	(*41*)	0.67 (0.35, 0.98)	4.19 x 10^{-11} M (1.07, 16.3) x 10^{-11}	2.81	0.98 (0.57, 1.39)	1.03 x 10^{-10} M (0.67, 1.6) x 10^{-10}	3.74
REGN10986[$]	Vero	VSV	9.91 x 10^{-11} M	(*41*)	0.81 (0.48, 1.14)	8.09 x 10^{-11} M (2.89, 22.7) x 10^{-11}	3.18	1.21 (0.62, 1.8)	1.82 x 10^{-10} M (1.16, 2.87) x 10^{-10}	4.31
REGN10987[$]	Vero	VSV	4.06 x 10^{-11} M	(*41*)	0.94 (0.74, 1.14)	5.69 x 10^{-11} M (3.03, 10.7) x 10^{-11}	3.82	1.15 (1.04, 1.25)	6.05 x 10^{-11} M (5.54, 6.61) x 10^{-11}	4.63
REGN10987	Calu-3	VSV	-	(*41*)	0.61 (0.55, 0.68)	1.71 x 10^{-11} M (1.06, 2.76) x 10^{-11}	2.82	0.65 (0.56, 0.74)	1.93 x 10^{-11} M (1.57, 2.37) x 10^{-11}	2.96
REGN10989	Vero	VSV	7.23 x 10^{-12} M	(*41*)	0.84 (0.5, 1.19)	7.60 x 10^{-12} M (3.52, 16.4) x 10^{-12}	4.17	0.94 (0.6, 1.29)	1 x 10^{-11} M (0.66, 1.52) x 10^{-11}	4.56
REGN10989	Calu-3	VSV	-	(*41*)	1.26 (1.09, 1.43)	7.85 x 10^{-12} M (6.22, 9.91) x 10^{-12}	6.21	1.19 (0.91, 1.48)	7.85 x 10^{-12} M (6.52, 9.45) x 10^{-12}	5.89
CC6.29[$*]	HeLa/ACE2	MLV	0.002 μg/ml	(*42*)	0.86 (0, 1.77)	0.003 μg/ml (0.0004, 0.02)	3.91	0.66 (0, 1.41)	0.002 μg/ml (0.0004, 0.01)	3.09
CC6.30[$]	HeLa/ACE2	MLV	0.0013 μg/ml	(*42*)	0.66 (0.33, 0.98)	0.001 μg/ml (0.0001, 0.002)	3.47	0.55 (0.21, 0.88)	0.001 μg/ml (0.0003, 0.003)	2.73

CC6.31*	HeLa/ACE2	MLV	0.059 μg/ml	(*42*)	0.41 (0, 1.45)	0.55 μg/ml (0.005, 64.13)	0.97	0.35 (0, 1.38)	0.71 μg/ml (0.0048, 105.98)	0.82
CC6.33	HeLa/ACE2	MLV	0.039 μg/ml	(*42*)	0.6 (0.37, 0.83)	0.02 μg/ml (0.01, 0.06)	2.27	0.66 (0.4, 0.93)	0.03 μg/ml (0.02, 0.06)	2.31
CC12.1*	HeLa/ACE2	MLV	0.019 μg/ml	(*42*)	1.14 (0, 2.85)	0.02 μg/ml (0.003, 0.14)	4.23	1.11 (0, 3.49)	0.02 μg/ml (0.002, 0.12)	4.18
CC12.3	HeLa/ACE2	MLV	0.018 μg/ml	(*42*)	1.02 (0.6, 1.43)	0.02 μg/ml (0.01, 0.05)	3.76	0.88 (0.64, 1.12)	0.02 μg/ml (0.01, 0.03)	3.28
CC12.4	HeLa/ACE2	MLV	0.11 μg/ml	(*42*)	0.95 (0.62, 1.28)	0.08 μg/ml (0.04, 0.18)	2.95	0.86 (0.49, 1.23)	0.11 μg/ml (0.06, 0.19)	2.55
CC12.14	HeLa/ACE2	MLV	0.023 μg/ml	(*42*)	0.79 (0.67, 0.91)	0.03 μg/ml (0.02, 0.04)	2.78	0.81 (0.7, 0.91)	0.04 μg/ml (0.03, 0.05)	2.76
ADI-55688$	HeLa/ACE2	MLV	-	(*35*)	0.45 (0.15, 0.74)	0.82 nM (0.07, 10.24)	1.32	0.81 (0.38, 1.23)	1.26 nM (0.62, 2.55)	2.2
ADI-55688	Vero	VSV	-	(*35*)	0.82 (0.6, 1.04)	0.37 nM (0.16, 0.84)	2.67	0.88 (0.45, 1.3)	0.46 nM (0.25, 0.83)	2.77
ADI-55689	HeLa/ACE2	MLV	-	(*35*)	0.72 (0.43, 1.01)	0.85 nM (0.28, 2.59)	2.08	0.79 nM (0.35, 1.22)	1.63 nM (0.74, 3.58)	2.06
ADI-55689	Vero	VSV	-	(*35*)	0.77 (0.47, 1.07)	0.16 nM (0.08, 0.32)	2.79	0.76 (0.27, 1.24)	0.14 nM (0.07, 0.31)	2.78
ADI-55690$	HeLa/ACE2	MLV	-	(*35*)	0.44 (0.12, 0.75)	0.64 nM (0.02, 20.49)	1.34	0.79 (0.1, 1.48)	4.48 nM (1.53, 13.08)	1.73
ADI-55690	Vero	VSV	-	(*35*)	0.73 (0.49, 0.96)	1.27 nM (0.48, 3.39)	1.98	0.65 (0.24, 1.06)	1.56 nM (0.58, 4.19)	1.72

ADI-55951[$]	HeLa/ACE2	MLV	-	(*35*)	0.24 (0.01, 0.48)	17.21 nM (0.01, 33973.11)	0.54	0.64 (0.13, 1.16)	10.46 nM (3.35, 32.72)	1.19
ADI-55951[$]	Vero	VSV	-	(*35*)	0.87 (0.37, 1.36)	2.33 nM (0.57, 9.49)	2.13	1.42 (0.56, 2.29)	5.03 nM (3.1, 8.15)	3.02
ADI-55993[$]	HeLa/ACE2	MLV	-	(*35*)	0.38 (0.15, 0.61)	0.31 nM (0.02, 6.48)	1.28	0.71 (0.28, 1.15)	0.68 nM (0.27, 1.72)	2.14
ADI-55993	Vero	VSV	-	(*35*)	1.04 (0.55, 1.53)	0.45 nM (0.19, 1.08)	3.31	0.99 (0.43, 1.55)	0.45 nM (0.26, 0.79)	3.15
ADI-56000[$]	HeLa/ACE2	MLV	-	(*35*)	0.43 (0.21, 0.65)	0.14 nM (0.01, 1.64)	1.6	0.92 (0.24, 1.6)	0.68 nM (0.29, 1.61)	2.74
ADI-56000	Vero	VSV	-	(*35*)	1.37 (0.76, 1.97)	0.75 nM (0.33, 1.71)	4.04	1.45 (0.52, 2.39)	0.61 nM (0.37, 1.02)	4.41
ADI-56010[$]	HeLa/ACE2	MLV	-	(*35*)	0.38 (0.15, 0.61)	0.25 nM (0.01, 4.9)	1.33	0.73 (0.28, 1.17)	1.55 nM (0.6, 3.97)	1.92
ADI-56010	Vero	VSV	-	(*35*)	1.15 (1.05, 1.25)	1.79 nM (1.46, 2.19)	2.95	1.13 (1.01, 1.24)	1.96 nM (1.78, 2.17)	2.85
ADI-56046	HeLa/ACE2	MLV	-	(*35*)	0.71 (0.38, 1.05)	0.86 nM (0.25, 2.95)	2.07	0.64 (0.24, 1.04)	1 nM (0.39, 2.56)	1.82
ADI-56046	Vero	VSV	-	(*35*)	1.54 (0.99, 2.09)	0.44 nM (0.25, 0.77)	4.9	1.41 (0.37, 2.44)	0.33 nM (0.19, 0.6)	4.64
COV21 IgG[$]	293T/ACE2	HIV-1	62.3 nM	(*43*)	1.44 (0.6, 2.28)	45.23 nM (17.3, 118.25)	1.69	1.22 (0.67, 1.78)	55.8 nM (37.04, 84.06)	1.34
COV57 IgG[*]	293T/ACE2	HIV-1	121.1 nM	(*43*)	1.25 (0, 4.85)	111.25 nM (3.66, 3384.5)	1.01	1.12 (0, 5.54)	128.92 nM (4.1, 4059.6)	0.86

S309[$]	VeroE6 or DBT/ACE2	MLV	-	(*44*)	0.91 (0.47, 1.34)	1.5 ng/ml (0.57, 3.94)	4.38	1.18 (0.71, 1.66)	1.08 ng/ml (0.75, 1.55)	5.89
S309[$]	VeroE6 or DBT/ACE2	MLV	-	(*44*)	0.85 (0.55, 1.14)	1.05 ng/ml (0.44, 2.51)	4.22	1.07 (0.64, 1.49)	0.5 ng/ml (0.33, 0.76)	5.65
Ty1-Fc	293T/ACE2	-	0.012 μg/ml	(*45*)	0.53 (0.46, 0.61)	0.02 μg/ml (0.01, 0.03)	1.96	0.57 (0.43, 0.72)	0.02 μg/ml (0.01, 0.03)	2.13
Ty1	293T/ACE2	-	0.77 μg/ml	(*45*)	0.84 (0.8, 0.88)	0.89 μg/ml (0.79, 1)	1.74	0.85 (0.77, 0.93)	0.83 (0.74, 0.94)	1.78

[$]NAbs ignored because IIP_{100} values estimated using Eqs. [1] and [2] deviated by 20% or more
[*]For 8 NAbs, the lower limit of 95% confidence interval was negative and was truncated to 0
[@]We assumed the molecular weight of NAbs to be 150 kDa for unit conversions
[#] IC_{50} values were digitized from Ref. (*6*)

Table S2: Viral dynamics model parameters and their values.

Parameter	Description	Value (Range)	Ref.
b	Infection rate constant of cells	6×10^{-8} virions^{-1} ml d^{-1} ($2.4 - 15.1) \times 10^{-8}$	(*24*)
r_X	Refractory state conversion rate constant	4 d^{-1} (3 - 5)	(*51*)
d	Infected cell death rate constant	0.6 d^{-1} (0.1 - 1.1)	(*25*)
p	Virion production rate per infected cell	390 virions ml^{-1} d^{-1} (290 - 490)	(*24*)
c	Virion clearance rate constant	20 d^{-1} (15 - 20)	(*24*)
s_X	Maximal innate immunity activation rate constant	1 d^{-1} (0.5 - 1.5)	(*51*)
f_X	Infected cell numbers at which innate immunity activation is half-maximal	100 cells (0.01 - 200)	(*51*)
d_X	Innate immunity decay rate constant	0.2 d^{-1} (0.15 - 0.25)	(*51*)
$T(0)$	Initial target cells	3×10^7 cells	Fixed
$I(0)$	Initial infected cells	1 cell	(*24*)
$V(0)$	Initial viral load	$\frac{pI(0)}{c}$	(*24*)
$X(0)$	Initial innate immune reponse (normalised value)	0	Fixed

[#]The ranges of parameter values used in simulations to account for inter-patient variations are indicated in parentheses

Table S3. Summary of clinical trials.

Vaccine	NT_{50} (95% CI)	Efficacy (95% CI)	Refs.
BNT162b2[*] (1 dose)[**]	14 (10 – 20)	49 (41 – 57)	(*55*, *56*)
BNT162b2[*] (2 doses)[***]	361 (235 – 550)	94 (87 – 97)	(*55*, *56*)
mRNA-1273[&] (2 doses)	356.2 (262.6 – 483.1)	95.6 (90.6 – 97.9)	(*1*, *57*)
ChAdOx1 nCoV-19[$] (2 doses)	239 (210 – 275)	80 (65.2 – 88.5)	*(58)*
Gam-COVID-Vac (Sputnik V)[#] (2 doses)	44.5 (31.8 – 62.2)	91.6 (85.6 – 95.2)	(*4*)

[*]NT_{50} measurements were from individuals aged between 18 and 55 years (*56*). Efficacy measurement included individuals aged between 16 and 39 years

[**]NT_{50} was measured on day 21 after 1st dose and efficacy was measured between days 14 and 21

[***]NT_{50} was measured on day 7 after 2nd dose (day 28 after 1st dose) and efficacy was measured 7 days after 2nd dose to end of the study

[#]NT_{50} was measured on day 42 after first dose and efficacy was measured from day 21 after 1st dose (the day of 2nd dose)

[&]NT_{50} measurements were from individuals aged between 18 and 55 years. Efficacy measurement included individuals aged between 18 and 65 years. NT_{50} values were digitized using Engauge 12.1.

[$]The interval between doses was ≥12 weeks. NT_{50} values were digitized using Engauge 12.1